Organic & Biomolecular Chemistry

Cite this: *Org. Biomol. Chem.*, 2011, **9**, 1565

www.rsc.org/obc

PAPER

An indole-linked C8-deoxyguanosine nucleoside acts as a fluorescent reporter of Watson–Crick *versus* Hoogsteen base pairing†

Katherine M. Schlitt,[a] Andrea L. Millen,[b] Stacey D. Wetmore*[b] and Richard A. Manderville*[a]

Received 14th October 2010, Accepted 22nd November 2010
DOI: 10.1039/c0ob00883d

Pyrrole- and indole-linked C^8-deoxyguanosine nucleosides act as fluorescent reporters of H-bonding specificity. Their fluorescence is quenched upon Watson–Crick H-bonding to dC, while Hoogsteen H-bonding to G enhances emission intensity. The indole-linked probe is ~ 10-fold brighter and shows promise as a fluorescent reporter of Hoogsteen base pairing.

Introduction

Fluorescence spectroscopy is a powerful bioanalytical tool. In nucleic acid chemistry, where the intrinsic fluorescence of DNA is very weak, it is common to label oligonucleotides with fluorescent probes for detection.[1] This strategy has many practical uses due to the high detection sensitivity of the fluorophore, yet is limited when applying fluorescence for study of DNA structure, dynamics and recognition, due to the bulk of the fluorophore coupled with its attachment to a flexible tether.[2] For these applications, fluorescent DNA base analogues that can mimic the structure and activity of the natural nucleobases and possess high fluorescence quantum yield sensitive to their local environment are ideal.[2,3]

Examples of fluorescent purine nucleoside analogues are shown in Fig. 1. In the first row, the heterocycles resemble the natural purine nucleobases and are minimally disruptive to DNA structure. The adenine analogue 2-aminopurine (2AP) is an example of an isomorphic base analogue with high fluorescence quantum yield (ϕ_{fl} = 0.68) that forms a stable Watson–Crick type base pair with thymine and a wobble base pair with cytosine.[4] The intensely fluorescent pteridines, 4-amino-6-methyl-pteridone (6MAP) and 6-methyl-isoxanthopterin (6MI) retain the Watson–Crick base pairing properties of adenine and guanine, respectively.[5] The fluorescence of 2AP, 6MAP and 6MI quenches when incorporated into oligonucleotides due to base-stacking interactions, making them useful as probes of environmental changes.[4,5] Replacement of C^8 in guanine with the more electronegative nitrogen generates 8-Aza-G that shows pH-dependent fluorescence with high quantum yield (ϕ_{fl} = 0.55) when N1 is deprotonated (pK_a = 8.05), but little fluorescence when N1 is protonated at neutral pH.[6] This deprotonation/protonation on/off fluorescence switching mechanism has been used as a reporter of the ionization state of active site guanines.[7]

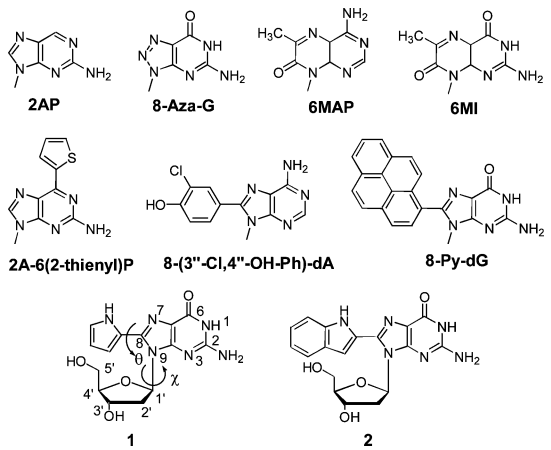

Fig. 1 Examples of fluorescent purine bases and structures, atomic numbering and identification of dihedral angles χ (∠(OC1′N9C4)) and θ (∠(C11C10C8N9)) for **1**.

The other purine bases shown in Fig. 1 are fluorophore-linked nucleotides, in which aromatic moieties are attached to 2AP (*i.e.* 2A-6(2-thienyl)P8) or the natural nucleobases. These types of fluorescent DNA base analogues can retain emission quantum efficiency upon incorporation into oligonucleotides and can expand the base pairing properties of the normal nucleobases.[8] Within this class of fluorophores, our group is interested in the properties of C^8-aryl(Ar)-purine adducts[9–12] that exhibit useful fluorescent properties.[13] Examples include 8-(3″-Cl,4″-OH-Ph)-dA that acts as a pH-sensing fluorescent probe at physiological pH[14] and 8-Py-dG that is a duplex-sensitive optical probe and a fluorescent donor for the investigation of charge transfer processes.[15]

Purine bases bearing C^8-heteroaryl derivatives are also of current interest because the heteroatoms can be used to increase

[a]*Departments of Chemistry and Toxicology, University of Guelph, Guelph, Ontario, Canada, N1G 2W1. E-mail: rmanderv@uoguelph.ca; Fax: 1-519-766-1499; Tel: 1-519-824-4120 53963*

[b]*Department of Chemistry and Biochemistry, University of Lethbridge, Lethbridge, Alberta, Canada, T1K 3M4. E-mail: stacey.wetmore@uleth.ca; Fax: 1-403-329-2057; Tel: 1-403-329-2323*

† Electronic supplementary information (ESI) available: NMR spectra of **1**, **2**, bissily**1** and bissilyl **2**, fluorescence emission titration data for bissilyl**1** (Figure S1) and Cartesian coordinates and absolute energies for all structures. See DOI: 10.1039/c0ob00883d

the number of H-bonds.[16] The Sessler laboratory has demonstrated that attachment of a pyrrole ring to the C^8-position of a guanine derivative results in a donor–acceptor–acceptor (DAA) motif, capable of forming a three-point extended Hoogsteen-type interaction with guanine involving the pyrrole NH functionality.[17] The Tor laboratory has also pointed out that purine bases bearing a C^8-furan are highly emissive ($\phi_{fl} \sim 0.6$).[18] This suggested that the pyrrole-dG analogue **1** may serve as a fluorescent probe for Hoogsteen base pairing, given the fluorescent nature of the corresponding furan analogue. A fluorescent probe that can distinguish Watson–Crick H-bonding from Hoogsteen H-bonding would be useful. Hoogsteen base pairs play a critical role in triplex[19] and quadruplex formation[20] and have been reported in protein/DNA complexes,[21] in RNA,[22] and in mismatches in DNA.[23] Hoogsteen DNA may also be an intermediate in a B-to-Z transition.[24]

To determine the potential utility of C^8-heteroaryl-dG derivatives to serve as fluorescent probes of Watson–Crick *vs.* Hoogsteen H-bonding, we have synthesized the pyrrole-linked derivative **1** and the corresponding indole-linked analogue **2** (Fig. 1) to initially characterize their structural, photophysical and redox properties. Both probes were expected to form stable Watson–Crick base pairs with dC and three-point Hoogsteen base pairs with G. Association reactions between **1** and **2** with G and dC carried out in $CHCl_3$ show these compounds to be useful fluorescent reporters of H-bonding specificity. Density functional theory (DFT) calculations on the structures of the modified bases, and on the Watson–Crick and Hoogsteen H-bond strengths between the *syn* or *anti* conformations of **1** and **2** have been employed to determine the potential role of base pairing in dictating their most favorable conformation in DNA helices. Our work represents the first step in developing these derivatives as fluorescent Hoogsteen base pairing probes. The favourable photophysical properties of the indole-linked probe **2** provides impetus for its further study in DNA duplex and triplex environments.

Results and discussion

Synthesis

The nucleosides **1** and **2** were synthesized from 8-Br-dG[25] and the appropriate boronic acids using a Suzuki–Miyaura cross-coupling reaction.[26] The probes **1** and **2** were also treated with $[(^i Pr)_2SiCl]_2O$ to modify the OH positions of the deoxyribose (dR) moiety and afford bissilyl derivatives that were soluble in $CHCl_3$. To establish association equilibria for base pairing in $CHCl_3$ using fluorescence spectroscopy, these modified bases were mixed with the corresponding bissilyl dC base for Watson–Crick H-bonding. The bissilyl dG base was not sufficiently soluble in $CHCl_3$, and so guanosine (G) bearing three *tert*-butyldimethylsilyl (TBDMS) protecting groups (G(TBDMS)$_3$) which is readily soluble in $CHCl_3$,[27] was prepared and used for analysis of Hoogsteen H-bonding by **1** and **2**.

Structure, photophysical and redox properties

Insight into the structural features of **1** and **2** was obtained from DFT calculations, as presented previously for various C^8-Ar-dG adducts.[10,12] For C^8-Ar-dG adducts bearing C^8-phenyl rings, *anti* structures are less stable than *syn* structures by ~25 kJ mol^{-1} and all *syn* minima contain an O5′–H $\cdots$ N3 hydrogen bond (1.80–1.96 Å).[10,12] The phenyl ring is also twisted with respect to the nucleobase, where the magnitude of the twist angle (θ) depends on steric considerations and favourable intramolecular interactions. For a phenyl ring and those bearing a *para* (*p*)-substituent, the global minima are twisted by ~37°, while the neutral nucleobase is planar ($\theta = 0°$), suggesting that the sugar moiety is inducing the twist within the nucleobase.[10,12] For a phenyl ring bearing an *ortho* (*o*)-substituent, θ increases to 45° for *o*-CH_3 and 55° for *o*-OCH_3 due to steric interactions.[12] In contrast, the global minimum for *o*-OH was less twisted ($\theta = 27°$) than for any other C^8-phenyl-dG adduct due to phenolic O–H $\cdots$ N^7 hydrogen bonding.[10,12]

Shown in Fig. 2 are DFT structures, geometrical parameters, and relative energies, for fully optimized minima and transition states for C^8-(1*H*-pyrrol-2-yl)-dG (**1**). Again, *syn* structures are more stable than *anti*, and contain an O$^{5'}$–H $\cdots$ N^3 hydrogen bond. The global minimum structure of **1** is only twisted by ~15° and the pyrrole NH is on the same H-bonding face as N^7. For the indole-linked derivative **2**, minimum energy structures from **1** were modified by the addition of the benzene ring and re-optimized. The minimum energy structures of **2** are the same as for the pyrrole probe **1**. The twist in the *syn* conformations is slightly different by 0–3° with the indole NH on the same H-bonding face as N^7.

Absorption and emission spectra for **1** and **2** were recorded in aqueous MOPS buffer, pH 7.0 (Fig. 3). Compared to the pyrrole-linked analogue **1**, the indole derivative **2** is ~ 10 times brighter and shows a bathochromic shift in absorbance. The electron-donor properties of the probes were determined using cyclic voltammetry in anhydrous DMF, as outlined previously for various C^8-Ar-dG analogues.[11] The nucleoside analogues showed irreversible 1-electron oxidation peaks with half-peak potentials ($E_{p/2}$) at 0.78 V/SCE for **1** and 0.89 V/SCE for **2**. Under these experimental conditions, dG gave $E_{p/2}$ = 1.14 V/SCE,[11] indicating that attachment of the heteroaromatic moiety enhances the electron-donor characteristics of the purine nucleoside. The optical and redox properties of the probes are given in Table 1.

Table 1 Photophysical and redox parameters for **1** and **2**

Probe	λ_{max} (nm), log ε^b	λ_{em} (nm),^{b} $\phi_{fl}{}^c$	brightness^d	$E_{p/2}{}^e$
1	292, 4.36	379, 0.10	2290	0.78
2	321, 4.48	390, 0.78	23600	0.89
dG^a	253, 4.14	334, 9.7×10^{-5}	1.33	1.14

^{a} Optical data for dG taken from Ref. 28 ^{b} Determined in aqueous 10 mM MOPS buffer, pH 7.0, $\mu = 0.1$ M NaCl. ^{c} Determined using the comparative method with quinine bisulfate in 0.5 M H_2SO_4 (ϕ_{fl} = 0.55). ^{d} Brightness calculated as $\varepsilon_{\lambda max}\phi_{fl}$. ^{e} Half-peak potentials in volts *vs.* SCE using cyclic voltammetry in 0.1 M TBAF in anhydrous DMF with a glassy carbon working electrode.

Association equilibria and H-bonding properties

The emissive properties of **1** and **2** prompted their testing as fluorescent reporters of H-bonding specificity. For these experiments, aprotic solvents, such as $CHCl_3$, are known to promote formation of H-bonded heterodimers.[29] Furthermore, the dielectric constant (ε = 4.9) of $CHCl_3$ is similar to that in the DNA double helix (ε = 3–5)[30] and serves as a reasonable model to study specific

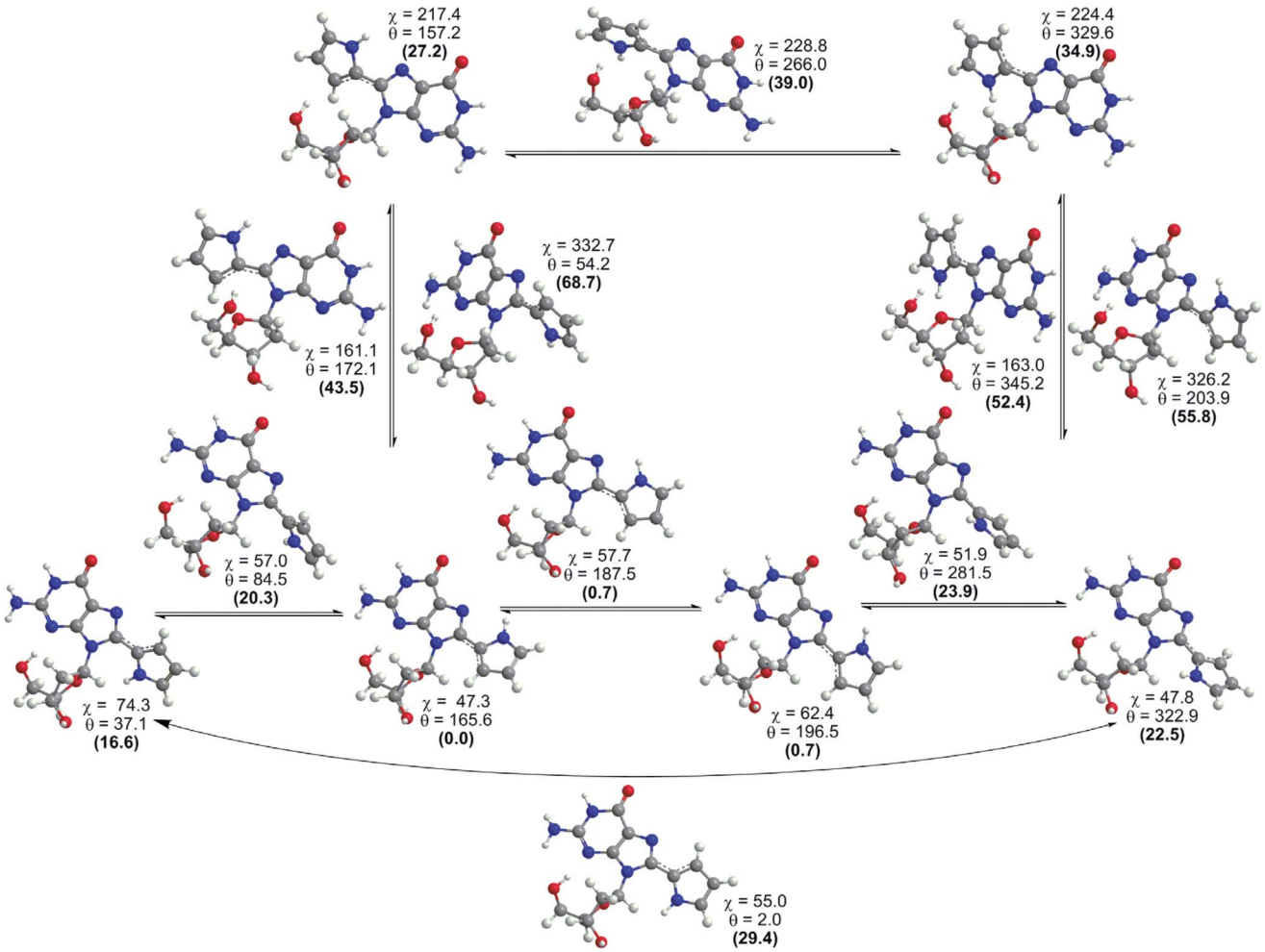

Fig. 2 Dihedral angles (χ and θ/deg) for the minima and transition states of C^8-(1*H*-pyrrol-2-yl)-dG (**1**) fully optimized with B3LYP/6-31G(d) (relative energies from B3LYP/6-311+G(2df,p) single-point calculations provided in parentheses, kJ mol^{-1}).

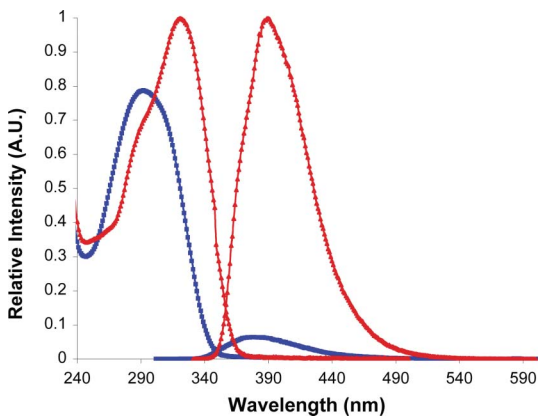

Fig. 3 Normalized absorption and emission spectra in pH 7 10 mM MOPS buffer, $\mu = 0.10$ M NaCl for probe **1**(□, blue) and **2** (△, red).

H-bonding effects in duplex DNA. For DNA duplexes in H_2O, dipole–dipole and π-stacking interactions may obscure or alter specific H-bonding effects.[31]

Thus, nucleosides **1** and **2** were treated with $[(^{i}Pr)_2SiCl]_2O$ to modify the OH positions of the deoxyribose (dR) moiety to afford bissilyl derivatives that are soluble in $CHCl_3$. Fluorescence spectroscopy was then used to establish association equilibria for Watson–Crick and Hoogsteen H-bonding by the bissilyl probes in $CHCl_3$ by mixing the probe with the corresponding bissilyl dC base and silyl-protected guanosine ($G(TBDMS)_3$).

Shown in Fig. 4 are changes in the fluorescence of bissilyl**2** upon addition of silyl-protected dC and G. Interestingly, addition of bissilyl dC caused ~ 4-fold decrease in the fluorescence intensity of bissilyl**2** (Fig. 4a), while in contrast addition of $G(TBDMS)_3$ caused a slight ~ 1.2-fold increase in fluorescence. For the weakly emissive bissilyl**1** similar trends were observed, with addition of bissilyl dC causing a 4-fold decrease in emission intensity and $G(TBDMS)_3$ causing a 1-fold increase in intensity (see the Electronic Supplementary Information (Figure S1) for fluorescence titrations with bissilyl**1**). Double reciprocal plots of $F_o/(F_o - F)$ as a function of 1/natural base concentration (inserts in Fig. 4) afforded straight lines, consistent with a 1 : 1 binding interaction. The association constant K_a was determined from the ratio of the intercept and slope and afforded a value of $(3.16 \pm 0.2) \times 10^4$ M^{-1} for the interaction of bissilyl**2** with bissilyl dC. The corresponding K_a value for bissilyl**1** with bissilyl dC was $(2.40 \pm 0.4) \times 10^4$ M^{-1}. Binding of bissilyl**2** with $G(TBDMS)_3$ afforded a K_a of $(1.38 \pm 0.2) \times 10^4$ M^{-1}; a K_a of $(1.29 \pm 0.95) \times 10^4$ M^{-1} was determined for bissilyl**1**.

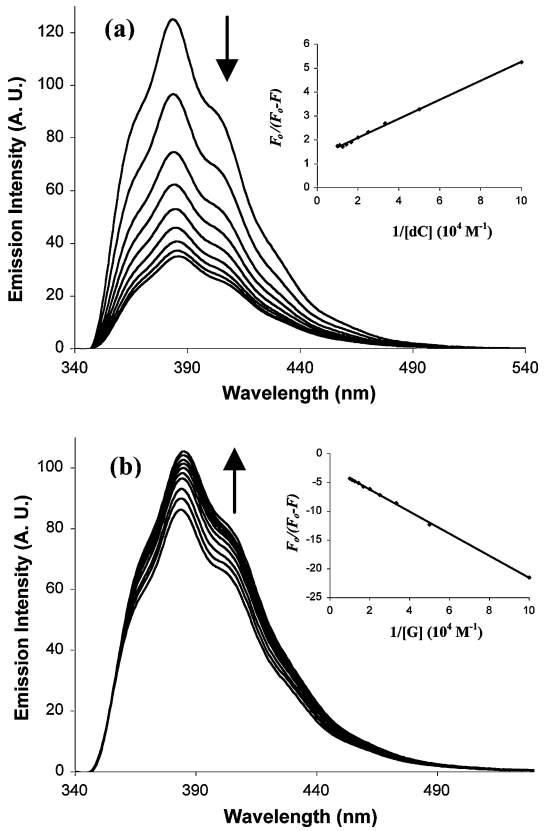

Fig. 4 Fluorescence emission titration of bissilyl**2** in $CHCl_3$ with (a) bissilyl dC and (b) $G(TBDMS)_3$.

Recently, Schwalb and coworkers[31] examined formation of H-bonded complexes between G:C and G:G in $CHCl_3$ using FTIR and determined a K_a value of $(3.4 \pm 0.8) \times 10^4$ M^{-1} for G:C formation. For the H-bridged dimer of G (G:G) the FTIR data favoured a two-point H-bonded reverse-Hoogsteen structure with a K_a of $(0.1 \pm 0.02) \times 10^4$ M^{-1}. Comparison to the fluorescence data indicates that the Watson–Crick binding strength is unaffected by the C^8-heteroaromatic, as the K_a values for **1**:dC and **2**:dC are within experimental error of K_a determined for G:C by FTIR. However, in terms of Hoogsteen binding to G, the C^8-heteroaryl moiety strengthens the interaction, as **1**:G and **2**:G would possess three H-bonds that would increase stability.[17] Furthermore, the G:G mismatch requires one base in the *anti* and the other in a *syn* conformation,[23] and both **1** and **2** prefer the *syn* conformation for further stabilization of the G:G mismatch.

Support for interpretation of the experimental data involving **1** and **2** was afforded by DFT calculations performed with Gaussian 03,[32] which provided information about both the structure and strength of the H-bonding interactions compared to the natural G:G and G:C base pairs. Structures of **1**:C, **1**:G, **2**:C and **2**:G base pairs are shown in Fig. 5, while binding strengths along with experimental K_a values are given in Table 2. The calculations also predict little influence of the C^8-heteroaryl group on Watson–Crick **1**:C and **2**:C, as the pyrrole and indole moieties are not involved in the interaction. The structures of **1**:G and **2**:G were modeled after the three-point Hoogsteen ensemble proposed for the pyrrole derivative involving an H-bond from the pyrrole NH atom to O^6 of G.[17] The probes **1** and **2** are present in the *syn* conformation and G remains in the *anti* orientation. These base pairs have a twisted geometry with an H-bond strength less than Watson–Crick G:C, but greater than normal G:G due to the extra H-bond contact.

Table 2 Association equilibria and hydrogen-bonding strengths for dimers involving natural DNA bases, **1** and **2**

Dimer	K_a ($\times 10^4$ M^{-1})[a]	ΔE_{HBond}[c] dR = H[d]	ΔE_{HBond}[c] dR = 2′-deoxyribose
G:C	3.4 ± 0.8[b]	–96.3	–94.6
G:G	0.101 ± 0.02[b]	–62.7	–61.7
1:dC	2.40 ± 0.4	–95.7	–96.1
1:G	1.29 ± 0.95	–81.0	–78.6
2:dC	3.16 ± 0.2	–96.7	–97.2
2:G	1.38 ± 0.2	–76.0	–74.3

[a] Recorded in $CHCl_3$ at room temperature. [b] Data taken from Ref. 31 [c] Relative energies in kJ mol^{-1} calculated at the B3LYP/6-311+G(2df,p)//B3LYP/6-31G(d,p) level of theory, and include ZPVE and BSSE corrections. [d] Deoxyribose was replaced with an H atom (dR = H).

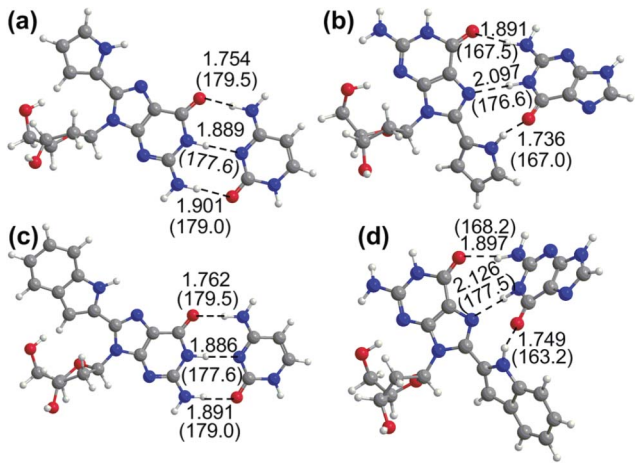

Fig. 5 Comparison of the structure of the H-bonded pairs optimized with B3LYP/6-31G(d,p) for (a) Watson–Crick **1**:C, (b) Hoogsteen **1**:G, (c) Watson–Crick **2**:C and (d) Hoogsteen **2**:G, with distances in Å and bond angles in deg. (parentheses).

Conclusions

In summary, the C^8-heteroaryl-dG nucleosides **1** and **2** exhibit fluorescence that is responsive to H-bonding interactions with dC and G. The fluorescence is quenched upon Watson–Crick H-bonding to dC, which is ascribed to a photoinduced electron transfer (PET) process from the excited-state fluorophore to the electron-accepting dC base.[33] In contrast, H-bonding of **1** and **2** with G enhances fluorescence intensity. The ability of **1** and **2** to form a three-point Hoogsteen complex with G would be expected to increase rigidity of the modified nucleoside, and hence increase fluorescence intensity. The indole-linked probe **2** is ~ 10 times brighter than the pyrrole-linked probe **1** with an excitation wavelength at 321 nm that is well separated from the absorption of DNA. Our work highlights the potential utility of **2** as a fluorescent base pairing probe and provides impetus for further study of **2** in DNA duplex and triplex environments.

Experimental

General

^{1}H NMR spectra were recorded on a Bruker Avance 300 DPX or Bruker Avance 400 DPX at 300.1 MHz and 400.1 MHz, respectively. ^{13}C NMR spectra were recorded on a Bruker Avance 300 DPX at 75.5 MHz. Unless specified all NMR experiments were carried out room temperature. ^{1}H NMR spectra were referenced to the residual proton solvent signal of the deuterated solvent and ^{13}C NMR spectra were referenced to the ^{13}C NMR resonance of the deuterated solvent. High-resolution mass spectra of probes **1**, **2**, bissilyl**1** and bissilyl**2** were conducted at the Biological Mass Spectrometry Facility (BMSF) at the University of Guelph and were obtained on a Waters Q-Tof operating in nanospray ionization at 0.5 uL min^{-1} detecting positive ions.

Unless otherwise noted, commercial compounds were used as received. Boronic acids were purchased from Sigma-Aldrich or Frontier Scientific, $Pd(OAc)_2$ from Sigma-Aldrich and 2′-deoxyguanosine (dG) from ChemGenes. Citric acid was purchased from Sigma-Aldrich and potassium dihydrogen phosphate from JT Baker Laboratory Chemicals. The synthesis of 8-bromo-2′-deoxyguanosine (8-Br-dG) was performed according to literature procedures by treating dG with *N*-bromosuccinimide in water–acetonitrile.[25]

UV-Vis spectra were recorded on a Cary 300-Bio UV-Visible Spectrophotometer equipped with a 6 × 6 Multicell Block Peltier, stirrer and temperature controller with Probe Series II. Fluorescence spectra were recorded on a Cary Eclipse Fluorescence Spectrophotometer equipped with a 1 × 4 Multicell Block Peltier, stirrer and temperature controller with Probe Series II. Standard 10 mm light path quartz glass cells from Hellma GmbH & Co. were used for both UV-Vis and fluorescence measurements. All UV-Vis and fluorescence spectra were recorded with baseline correction and stirring at room temperature. For all spectroscopic measurements, excitation and emission slit widths were kept constant at 2.5 nm. Stock solutions of **1** and **2** were prepared in DMSO due to sparing solubility in other solvents. Any water used for buffers or spectroscopic solutions was obtained from a MilliQ filtration system (18.2 MΩ). pH measurements were taken at room temperature with an Accumet 910 pH meter with an Accumet pH Combination Electrode with stirring. Electrochemical oxidation measurements were conducted using an Autolab PGSTAT30 potentiostat instrument, and electrodes polished with LECO Microid Diamond using the Spectrum System 1000.

Suzuki coupling of 8-Br-dG with boronic acids

These reactions were conducted according to the literature[26] and are briefly described here. Palladium acetate (2.2 mg, 0.01 mmol), tris-(2-sulfophenyl)phosphine trisodium salt (TPPTS) (14.8 mg, 0.025 mmol), sodium carbonate (80 mg, 0.75 mmol), 8-Br-dG (0.375 mmol), and the appropriate boronic acid (0.45 mmol) were added to degassed 2 : 1 water–acetonitrile (3.5 mL) and heated to 80 °C for 4 h under an argon atmosphere. The reaction was diluted with *ca.* 20 mL of water and the pH adjusted to 6–7 with 1 M HCl (aq). The mixture was allowed to cool to 0 °C for several hours before the product was recovered by vacuum filtration.

8-(2″-Pyrrolyl)-2′-deoxyguanosine (1). Starting from 8-Br-dG (147.5 mg, 0.4261 mmol), 1-(*t*-butoxycarbonyl)-pyrrole-2-boronic acid (178.7 mg, 0.8468 mmol), $Pd(OAc)_2$ (5.1 mg, 0.023 mmol), TPPTS (13.0 mg, 0.0220 mmol), and Na_2CO_3 (97.9 mg, 0.917 mmol), adduct **1** was obtained as a light grey solid (102.1 mg, 72.1%). UV-vis (pH 7) λ_{max} 292, ε_{292} 22 909 cm^{-1} M^{-1}; ^{1}H NMR (DMSO-d_6) (300 MHz), δ: 11.57 (s, 1H), 10.67 (s, 1H), 6.89 (s, 1H), 6.47 (s, 1H), 6.32 (m, 3H), 6.18 (d, J = 2.7 Hz, 1H), 5.17 (d, J = 4.2 Hz, 1H), 5.03 (t, J = 5.6 Hz, 1H), 4.39 (bs, 1H), 3.81 (bs, 1H), 3.64 (m, 1H), 3.55 (m, 1H), 3.23 (m, 1H), 2.08 (m, 1H); ^{13}C NMR (DMSO-d_6) (75.5 MHz), δ: 156.6, 152.8, 151.8, 141.6, 120.8, 120.8, 116.9, 109.9, 108.9, 87.8, 84.6, 71.2, 62.1, 36.7; HRMS calcd for $C_{14}H_{16}N_6O_4$ [M + H$^+$] 333.1311, found 333.1301.

8-(2″-Benzopyrrolyl)-2′-deoxyguanosine (2). Starting from 8-Br-dG (128.0 mg, 0.3698 mmol), 1-*N*-Boc-indole-2-boronic acid (352.0 mg, 1.348 mmol), $Pd(OAc)_2$ (4.3 mg, 0.020 mmol), TPPTS (16.7 mg, 0.0282 mmol), and Na_2CO_3 (80.7 mg, 0.756 mmol), adduct **2** was recovered as a grey solid, following extraction with $CHCl_3$ (3×) to remove the 1-*N*-Boc-indole-2-boronic acid impurity (88.3 mg, 62.4%). UV-vis (pH 7) λ_{max} 321, ε_{278} 30, 130 cm^{-1} M^{-1}; ^{1}H NMR (DMSO-d_6) (300 MHz), δ: 11.76 (s, 1H), 10.80 (s, 1H), 7.62 (d, J = 7.8 Hz, 1H), 7.43 (d, J = 8.1 Hz, 1H), 7.15 (t, J = 7.5 Hz, 1H), 7.03 (t, J = 7.2 Hz, 1H), 6.88 (s, 1H), 6.45 (m, 3H), 5.21 (d, J = 4.2 Hz, 1H), 5.04 (t, J = 5.2 Hz, 1H), 4.43 (bs, 1H), 3.86 (bs, 1H), 3.68 (m, 1H), 3.57 (m, 1H), 3.26 (m, 1H), 2.12 (m, 1H); ^{13}C NMR (DMSO-d_6) (75.5 MHz), δ: 156.7, 153.1, 152.2, 140.7, 136.6, 127.7, 127.0, 122.6, 120.6, 119.6, 117.3, 111.7, 102.5, 87.8, 84.5, 71.0, 61.9, 36.6; HRMS calcd for $C_{18}H_{18}N_6O_4$ [M + H$^+$] 383.1423, found 383.1432.

Silylation reactions

These reactions were conducted according to the literature[34] and are briefly described here. The probes **1**, **2** or dC and imidazole were added in a 5 : 1 ratio to 5 mL of anhydrous DMF, and the reaction mixture was cooled to 0 °C. The reaction mixture was treated with excess 1,3-dichloro-1,1,3,3-tetraisopropyldisiloxane ([(*i*Pr)$_2$SiCl]$_2$O), and then warmed to room temperature and stirred under an argon atmosphere overnight. The product was precipitated upon the addition of approximately 25 mL of water and collected by vacuum filtration. The products were purified by flash chromatography on silica, eluting with 9 : 1 $CHCl_3$–MeOH. Bissilyl dC was prepared as described above and spectra obtained matched the published ^{1}H NMR and ^{13}C NMR data.[35] The synthesis of 2′,3′,5′-tris((*tert*-butyldimethylsilyl)oxy) guanosine (G(TBDMS)$_3$) was conducted according to the literature.[27] Guanosine, TBDMSCl and imidazole were added in a 1 : 6.6 : 13.2 ratio to 5 mL of anhydrous DMF, and the reaction mixture was stirred at room temperature under an argon atmosphere overnight. The product was precipitated upon the addition of approximately 25 mL of water and collected by vacuum filtration. The products were purified by flash chromatography on silica, eluting with 9 : 1 $CHCl_3$–MeOH. Spectrum obtained matched the published ^{1}H NMR data.[36]

8-(2″-Pyrrolyl)-3′,5′-*O*-(1,1,3,3-tetraisopropyldisiloxane-1,3-diyl)-2′-deoxyguanosine (bissilyl1). Starting from **1** (49.3 mg, 0.148 mmol), imidazole (76.5 mg, 1.12 mmol), and ([(*i*Pr)$_2$SiCl]$_2$O

(0.10 mL, 0.31 mmol), bissilyl**1** was obtained as a white solid (21.1 mg, 24.1%). ^{1}H NMR (DMSO-d_6) (300 MHz), δ: 11.61 (bs, 1H), 10.78 (s, 1H), 6.91 (s, 1H), 6.52 (s, 1H), 6.28 (q, J = 4.3 Hz, 1H), 6.15 (s, 1H), 6.01 (s, 2H), 4.87 (q, J = 5.7 Hz, 1H), 3.95 (m, 1H), 3.82 (m, 2H), 3.22 (m, 1H), 2.30 (m, 1H), 1.19–0.95 (m, 28H); HRMS calcd for $C_{26}H_{42}N_6O_5Si_2$ [M + H$^+$] 575.2828, found 575.2823.

8-(2″-Benzopyrrolyl)-3′,5′-*O*-(1,1,3,3-tetraisopropyldisiloxane-1,3-diyl)-2′-deoxyguanosine (bissilyl2). Starting from **2** (52.0 mg, 0.136 mmol), imidazole (82.1 mg, 1.21 mmol), and ([(*i*Pr)$_2$SiCl]$_2$O (0.10 mL, 0.31 mmol), bissilyl**2** was obtained as a white solid (47.6 mg, 54.8%). ^{1}H NMR (CD_2Cl_2) (300 MHz), δ: 12.01 (bs, 1H), 10.53 (bs, 1H), 7.70 (d, J = 7.8 Hz, 1H), 7.47 (d, J = 8.1 Hz, 1H), 7.28 (t, J = 8.1 Hz, 1H), 7.17 (m, 2H), 6.48 (d, J = 7.5 Hz, 1H), 5.88 (bs, 2H), 5.34 (m, 1H), 4.09 (m, 1H), 4.02 (m, 2H), 3.45 (bs, 1H), 2.48 (m, 1H), 1.19–0.93 (m, 28H); HRMS calcd for $C_{30}H_{44}N_6O_5Si_2$ [M + H$^+$] 625.2984, found 625.2970.

Determination of photophysical properties

Stock solutions of adducts **1** and **2** were made in DMSO to a concentration of 4 mM. Spectroscopic solutions were prepared with 5 μL of stock solution and 1995 μL of 10 mM MOPS (pH 7.0, μ = 0.1 M NaCl). UV-Vis spectral measurements were observed from 220 to 400 nm, with fluorescence spectra recorded at the excitation wavelength (absorbance maxima) for the probe of interest, from 10 nm above the excitation wavelength to 600 nm.

Quantum yield measurements

Quantum yield values for adducts **1** and **2** were determined in 10 mM MOPS buffer (pH 7.0, μ = 0.1 M NaCl) using the comparative method.[37] Quinine bisulfate (ϕ_{fl} = 0.546) in 0.5 M H_2SO_4 was used as the fluorescence quantum yield standard.[38] The following equation was used to calculate fluorescence quantum yields: $\phi_{fl}(x) = (A_s/A_x)(F_x/F_s)(\eta_x/\eta_s)^2\phi_{fl}(s)$ where s is the standard, x is the unknown, A is the absorbance at the excitation wavelength, F is the integrated area under the emission curve, η is the refractive index of the solvent and ϕ_{fl} is the quantum yield. The refractive index corrective term was not included due to the similar refractive indices of H_2O and 0.5 M H_2SO_4. Excitation and emission slit-widths were kept constant for all fluorescence measurements at 2.5 nm. Absorbance readings were kept below 0.06 to avoid inner-filter and self-absorbance phenomena.

Cyclic voltammetry (CV)

Electrochemical oxidation measurements were conducted in a three-electrode glass cell under nitrogen. Measurements were carried out in a solution of 0.1 M DMF/TBAF. The working electrode used was glassy carbon, 2 mm in diameter. The electrode was polished and ultrasonically rinsed with ethanol. A silver wire placed in a 0.1 M DMF/TBAF solution was used as the reference electrode, and was separated from the main solution by a fine porosity frit. The reference electrode potential was calibrated *in situ* against 1 mol equiv of 9,10-anthraquinone (–0.800 V *vs.* SCE). The counter electrode used was platinum wrapped in foil. For all CV's, the starting potential was 0 V, and the potential was first scanned 1.8 V towards positive potentials, and then scanned 1.8 V towards negative potentials. The scanning rate used was 0.2 V s^{-1}. Peak picking was achieved by correlation of values obtained from automatic software methods and manual assignment.

Association equilibrium constant determination

Binding constants were determined by fluorescence spectrophotometry using only silylated derivatives. Stock solutions of bissilyl**1** and bissilyl**2** were prepared in $CHCl_3$ to a concentration of 4 mM. Stock solutions of bissilyl dC and G(TBDMS)$_3$ were prepared in $CHCl_3$ to a concentration of 10 mM. Spectroscopic solutions were prepared with 5 μL of bissilylated probe stock solution and 1993 μL of $CHCl_3$. The stock solution of either bissilyl dC or G(TBDMS)$_3$ was then titrated in 2 μL increments into the spectroscopic solution until no further change was observed in fluorescence intensity. This procedure was conducted in triplicate, allowing for determination of an average K_a value for each dimer system. The association equilibrium constant K_a was determined from the ratio of the intercept and the slope from the double reciprocal plot of $F_o/(F_o - F)$ *vs.* 1/[titrant].[39]

Computational details

The minima of **1** and **2** were identified by full optimizations at the B3LYP/6-31G(d) level of theory. Accurate relative energies were calculated at the B3LYP/6-311+G(2df,p) level of theory including scaled (0.9806)[40] zero-point vibrational energy corrections. The Watson–Crick and Hoogsteen hydrogen-bonded complexes formed between guanine and either cytosine or guanine, and **1** and **2** with either cytosine or guanine, were optimized in the gas phase with B3LYP/6-31G(d,p). Two computational models were used for the base pairs: 1) the nucleobase model, where the DNA sugar moiety was replaced with a hydrogen atom for both the modified and the natural bases (dR = H), and 2) the nucleoside model, where a deoxyribose unit was attached to the modified base (or natural guanine for comparison) and a hydrogen atom replaced the sugar moiety in the natural base (dR = 2′-deoxyribose). B3LYP/6-311+G(2df,p) single-point calculations were performed to obtain accurate binding energies, which also include counterpoise corrections to account for the basis set superposition error (BSSE) and scaled (0.9806)[40] zero-point vibrational energy corrections. The interaction energies were calculated as the difference between the energy of the optimized complex and the sum of the energies of the individually optimized monomers. The conformation of the (G, **1** or **2**) nucleoside monomers (*anti* or *syn*) corresponds to the conformation in the optimized (Watson–Crick or Hoogsteen) hydrogen-bonded complex. All calculations were performed using Gaussian 03.[32]

Acknowledgements

Support for this research was provided by the Natural Sciences and Engineering Research Council (NSERC) of Canada, the Canada Research Chair program, the Canada Foundation for Innovation, and the Ontario Innovation Trust Fund. ALM thanks Alberta Ingenuity, now part of Alberta Innovates-Technology Futures, and NSERC for funding.

Notes and references

1 (*a*) C. Wojczewski, K. Stolze and J. W. Engels, *Synlett*, 1999, 1667–1678; (*b*) R. T. Ranasinghe and T. Brown, *Chem. Commun.*, 2005, 5487–5502; (*c*) A. P. Silverman and E. T. Kool, *Chem. Rev.*, 2006, **106**, 3775–3789.
2 J. N. Wilson and E. T. Kool, *Org. Biomol. Chem.*, 2006, **4**, 4265–4274.
3 R. W. Sinkeldam, N. J. Greco and Y. Tor, *Chem. Rev.*, 2010, **110**, 2579–2619.
4 (*a*) D. C. Ward, E. Reich and L. Stryer, *J. Biol. Chem.*, 1969, **244**, 1228–1237; (*b*) J. M. Jean and K. B. Hall, *Proc. Natl. Acad. Sci. U. S. A.*, 2001, **98**, 37–41; (*c*) E. L. Rachofsky, R. Osman and J. B. A. Ross, *Biochemistry*, 2001, **40**, 946–956.
5 (*a*) M. E. Hawkins, W. Pfleiderer, A. Mazumder, Y. G. Pommier and F. M. Balis, *Nucleic Acids Res.*, 1995, **23**, 2872–2880; (*b*) M. E. Hawkins, W. Pfleiderer, O. Jungmann and F. M. Balis, *Anal. Biochem.*, 2001, **298**, 231–240.
6 (*a*) J. Wierzchowski, B. Wielgus-Kutrowska and D. Shugar, *Biochim. Biophys. Acta*, 1996, **1290**, 9–17; (*b*) F. Seela, D. Jiang and K. Xu, *Org. Biomol. Chem.*, 2009, **7**, 3463–3473.
7 C. P. Da Costa, M. J. Fedor and L. G. Scott, *J. Am. Chem. Soc.*, 2007, **129**, 3426–3432.
8 (*a*) I. Hirao, Y. Harada, M. Kimoto, T. Mitsui, T. Fujiwara and S. Yokoyama, *J. Am. Chem. Soc.*, 2004, **126**, 13298–13305; (*b*) T. Mitsui, M. Kimoto, R. Kawai, S. Yokoyama and I. Hirao, *Tetrahedron*, 2007, **63**, 3528–3537; (*c*) S. G. Srivatsan and Y. Tor, *J. Am. Chem. Soc.*, 2007, **129**, 2044–2053.
9 C. K. McLaughlin, D. R. Lantero and R. A. Manderville, *J. Phys. Chem. A*, 2006, **110**, 6224–6230.
10 (*a*) A. L. Millen, C. K. McLaughlin, K. M. Sun, R. A. Manderville and S. D. Wetmore, *J. Phys. Chem. A*, 2008, **112**, 3742–3753; (*b*) A. L. Millen, R. A. Manderville and S. D. Wetmore, *J. Phys. Chem. B*, 2010, **114**, 4373–4382; (*c*) A. L. Millen, C. D. M. Churchill, R. A. Manderville and S. D. Wetmore, *J. Phys. Chem. B*, 2010, **114**, 12995–13004.
11 J. L. Weishar, C. K. McLaughlin, M. Baker, W. Gabryelski and R. A. Manderville, *Org. Lett.*, 2008, **10**, 1839–1842.
12 K. M. Schlitt, K. M. Sun, R. J. Paugh, A. L. Millen, L. Navarro-Whyte, S. D. Wetmore and R. A. Manderville, *J. Org. Chem.*, 2009, **74**, 5793–5802.
13 A. Collier and G. K. Wagner, *Chem. Commun.*, 2008, 178–180.
14 K. M. Sun, C. K. McLaughlin, D. R. Lantero and R. A. Manderville, *J. Am. Chem. Soc.*, 2007, **129**, 1894–1895.
15 (*a*) L. Valis, E. Mayer-Enthart and H.-A. Wagenknecht, *Bioorg. Med. Chem. Lett.*, 2006, **16**, 3184–3187; (*b*) C. Wanninger-Weiß, L. Valis and H.-A. Wagenknecht, *Bioorg. Med. Chem.*, 2008, **16**, 100–106.
16 G. Hobley, V. Gubala, M. D. C Rivera-Sánchez and J. M. Rivera, *Synlett*, 2008, 1510–1514.
17 J. L. Sessler, J. Jayawickramarajah, C. L. Sherman and J. S. Brodbelt, *J. Am. Chem. Soc.*, 2004, **126**, 11460–11461.
18 N. J. Greco and Y. Tor, *Tetrahedron*, 2007, **63**, 3515–3527.
19 Y. Wang, D. A. Rusling, V. E. C. Powers, O. Lack, S. D. Osborne, K. R. Fox and T. Brown, *Biochemistry*, 2005, **44**, 5884–5892.
20 J. T. Davis and G. P. Spada, *Chem. Soc. Rev.*, 2007, **36**, 296–313.
21 (*a*) G. A. Patikoglou, J. L. Kim, L. Sun, S.-H. Yang, T. Kodadek and S. K. Burley, *Genes Dev.*, 1999, **13**, 3217–3230; (*b*) M. Kitayner, H. Rozenberg, R. Rohs, O. Suad, D. Rabinovich, B. Honig and Z. Shakked, *Nat. Struct. Mol. Biol.*, 2010, **17**, 423–429.
22 E. I. Zagryadskaya, F. R. Doyon and S. V. Steinberg, *Nucleic Acids Res.*, 2003, **31**, 3946–3953.
23 J. V. Skelly, K. J. Edwards, T. C Jenkins and S. Neidle, *Proc. Natl. Acad. Sci. U. S. A.*, 1993, **90**, 804–808.
24 N. G. A. Abrescia, A. Thompson, T. Huynh-Dinh and J. A. Subirana, *Proc. Natl. Acad. Sci. U. S. A.*, 2002, **99**, 2806–2811.
25 (*a*) P. M. Gannett and T. P. Sura, *Synth. Commun.*, 1993, **23**, 1611–1615; (*b*) L. Gillet and O. D. Schärer, *Org. Lett.*, 2002, **4**, 4205–4208.
26 E. C Western, J. R. Daft, E. M. Johnson, II, P. M Gannett and K. H. Shaughnessy, *J. Org. Chem.*, 2003, **68**, 6767–6774.
27 K. K. Ogilvie, *Can. J. Chem.*, 1973, **51**, 3799–3807.
28 D. Onidas, D. Markovitsi, S. Marguet, A. Sharonov and T. Gustavsson, *J. Phys. Chem. B*, 2002, **106**, 11367–11374.
29 Y. Kyogoku, R. C. Lord and A. Rich, *Science*, 1966, **154**, 518–520.
30 K. Siriwong, A. A. Voityuk, M. D. Newton and N. Rösch, *J. Phys. Chem. B*, 2003, **107**, 2595–2601.
31 N. K. Schwalb, T. Michalak and F. Temps, *J. Phys. Chem. B*, 2009, **113**, 16365–16376.
32 *Gaussian 03*, Revision D.02, M. J. Frisch, G. W. Trucks, H. B. Schlegel, G. E. Scuseria, M. A. Robb, J. R. Cheeseman, J., J. A. Montgomery, T. Vreven, K. N. Kudin, J. C. Burant, J. M. Millam, S. S. Iyengar, J. Tomasi, V. Barone, B. Mennucci, M. Cossi, G. Scalmani, N. Rega, G. A. Petersson, H. Nakatsuji, M. Hada, M. Ehara, K. Toyota, R. Fukuda, J. Hasegawa, M. Ishida, T. Nakajima, Y. Honda, O. Kitao, H. Nakai, M. Klene, X. Li, J. E. Knox, H. P. Hratchian, J. B. Cross, V. Bakken, C. Adamo, J. Jaramillo, R. Gomperts, R. E. Stratmann, O. Yazyev, A. J. Austin, R. Cammi, C. Pomelli, J. W. Ochterski, P. Y. Ayala, K. Morokuma, G. A. Voth, P. Salvador, J. J. Dannenberg, V. G. Zakrzewski, S. Dapprich, A. D. Daniels, M. C. Strain, O. Farkas, D. K. Malick, A. D. Rabuck, K. Raghavachari, J. B. Foresman, J. V. Ortiz, Q. Cui, A. G. Baboul, S. Clifford, J. Cioslowski, B. B. Stefanov, G. Liu, A. Liashenko, P. Piskorz, I. Komaromi, R. L. Martin, D. J. Fox, T. Keith, M. A. Al-Laham, C. Y. Peng, A. Nanayakkara, M. Challacombe, P. M. W. Gill, B. Johnson, W. Chen, M. W. Wong, C. Gonzalez and J. A. Pople, Gaussian Inc., Wallingford CT, 2004.
33 (*a*) Y. J. Seo, J. H. Ryu and B. H. Kim, *Org. Lett.*, 2005, **7**, 4931–4933; (*b*) A. T. Krueger and E. T. Kool, *J. Am. Chem. Soc.*, 2008, **130**, 3989–3999.
34 L. V. Nechev, I. D. Kozekov, A. K. Brock, C. J. Rizzo and T. M. Harris, *Chem. Res. Toxicol.*, 2002, **15**, 607–613.
35 A. B. Sierzchala, D. J. Dellinger, J. R. Betley, T. K. Wyrzykiewicz, C. M. Yamada and M. H. Caruthers, *J. Am. Chem. Soc.*, 2003, **125**, 13427–13441.
36 C. S. Foote and C. Sheu, *J. Am. Chem. Soc.*, 1995, **117**, 6439–6442.
37 S. Fery-Forgues and D. Lavabre, *J. Chem. Educ.*, 1999, **76**, 1260–1264.
38 J. N. Demas and G. A. Crosby, *J. Phys. Chem.*, 1971, **75**, 991–1024.
39 S. Dubeau, P. Bourassa, T. J. Thomas and H. A. Tajmir-Riahi, *Biomacromolecules*, 2010, **11**, 1507–1515.
40 A. P. Scott and L. Radom, *J. Phys. Chem.*, 1996, **100**, 16502–16513.